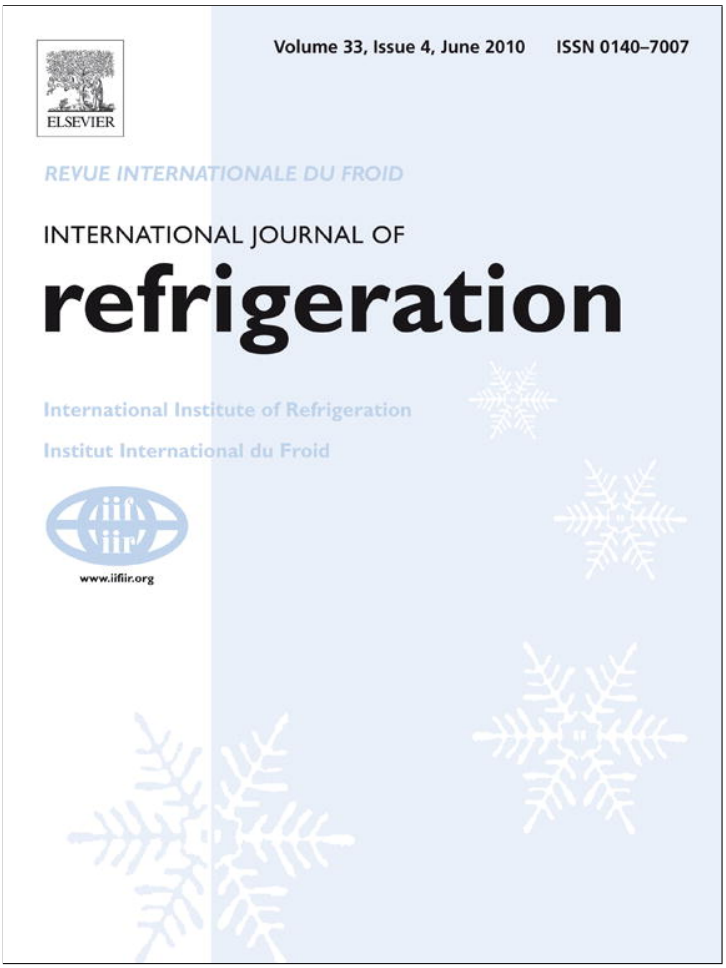

INTERNATIONAL JOURNAL OF REFRIGERATION 33 (2010) 793–805

available at www.sciencedirect.com

ScienceDirect

journal homepage: www.elsevier.com/locate/ijrefrig

Experimental study and modeling of cooling ceiling systems using steady-state analysis

Néstor Fonseca Diaz [a,b,*], Jean Lebrun [a], Philippe André [c]

[a] Thermodynamic Laboratory, University of Liège Belgium, Campus du Sart Tilman, Bât: B49 – P33, B-4000 Liège, Belgium
[b] Universidad Tecnológica de Pereira, Facultad de Ingeniería Mecùanica, AA. 97 Pereira, Colombia
[c] Département Sciences et Gestion de l'Environnement, University of Liège Belgium, 185, Avenue de Longwy, B-6700 Arlon, Belgium

ARTICLE INFO

Article history:
Received 7 February 2009
Received in revised form
3 December 2009
Accepted 12 December 2009
Available online 4 January 2010

Keywords:
Air conditioning Experiment
Geometry
Coil
Cooling
Ceiling
Modelling

ABSTRACT

This article presents the results of an experimental study performed to develop a computational model of cooling ceiling systems. The model considers the cooling ceiling as a fin. Only the dry regime is considered. From ceiling and room dimensions, material description of the cooling ceiling and measurement of supply water mass flow rate and air and water temperatures, the model calculates the cooling ceiling capacity, ceiling surface average temperature and water exhaust temperature. Fin efficiency, mixed convection close to the cooling ceiling (generated by the ventilation system) and panel perforations influence are studied. The theoretical approach gives to the user an appropriate tool for preliminary calculation, design and diagnosis in commissioning processes in order to determine the main operating conditions of the system in cooling mode. A series of experimental results got on four types of cooling ceilings are used in order to validate the model.

Titre Etude expérimentale et modélisation des systèmes de plafond refroidissant à l'aide d'une analyse du régime permanent

Mots clés : Conditionnement d'air ; Expérimentation ; Géométrie ; Serpentin ; Refroidissement ; Plafond ; Modélisation

1. Introduction

Cooling ceilings systems have been used for many years in commercial applications, with a high percentage of sensible heat removed and low energy consumption. While the primary air distribution is used to fulfill the ventilation requirements, the secondary water distribution system provides thermal conditioning to the building. According to

* *Corresponding author*. Universidad Tecnológica de Pereira, Facultad de Ingeniería Mecánica,Pereira, Colombia. Tel.: +57 6 3137124.
E-mail address: nfonseca@utp.edu.co (N. Fonseca Diaz).
0140-7007/$ – see front matter
doi:10.1016/j.ijrefrig.2009.12.011

Nomenclature

A	area, [m^2]
AU	heat transfer coefficient, W K^{-1}
C	factor, [–]
c	specific heat, [J kg^{-1} K^{-1}]
D	diameter [m]
h	superficial (convection and/or radiation) heat transfer coefficient, [W m^{-2} K^{-1}]
k	thermal conductivity[W m^{-1} K^{-1}]
L	length [m]
$\dot{M}$	mass flow rate, [kg s^{-1}]
N	number [–]
NTU	number of transfer units, [–]
P	pressure or perimeter, [Pa] or [m]
$\dot{Q}$	heat flow, [W]
$\dot{Q}'$	heat flow per unit length, [W m^{-1}]
$\dot{q}$	heat flow density, [W m^{-2}]
R'	thermal resistance per unit length, [K m W^{-1}]
t	temperature, [°C]
U	overall heat transfer coefficient, [W m^{-2} K^{-1}]
w	distance between tubes[m]

Dimensionless numbers

Nus	Nusselt number, [–]
Pr	Prandtl number, [–]
Ra	Rayleigh number, [–]
$Re_{D,L}$	Reynolds number, [–]

Greek symbols

ε	effectiveness or emissivity, [–]
δ	thickness, [m]
ρ	density or ceiling panel porosity factor, [kg m^{-3}] or [–]
Δ_T	temperature difference, [K]
θ	error function, [–]
μ	dynamic viscosity, [Pa. s]

Subscripts

a	air
b	distance between tube axis and ceiling surface
c	characteristic or cross-sectional
cc	cooling ceiling
comb	combined forced an natural convection
conv	convective
e	external
ex	exhaust
exp	experimental
f	fictitious, fin
i	internal
meas	measured
mr	mean radiant
p	panel or panels blocks connected in parallel
rad	radiative
res	resultant
su	supply
s	panels connected in series or surface
sim	simulated
t	tube
w	water
x	fin distance
0	fin base

Conroy and Mumma (2005), cooling ceiling systems significantly reduce the amount of air transported through the building (often only about 20% of the normal all-air system air flow rates). This results in the reduction of the fan size, energy consumption and ductwork cross-sectional dimensions (Feustel and Stetiu, 1995).

Due to the large surface available for heat exchange, the water temperature is only slightly lower than the room temperature; this small difference allows the use of either heat pump with very high coefficient of performance, or alternative cooling sources. Some problems as water piping in ceiling directly above the workplace, with attendant fears of possible leakage, condensation, unpleasant coldness, etc. have generally given way to a high level of acceptance.

Today, there is an increasing interest to extend the range of application to heating, in order to save on investment costs on one hand, and on the other one to avoid the use of static heaters under or in front of glass facades, which are often undesirable for architectural reasons. However, it is important to remark, that the commissioning process is especially important in this system to detection and diagnosis of a possible malfunction of the system.

This article summarizes an experimental investigation and the modeling of two cooling ceiling systems with four different configurations.

2. Experimental description

The system is studied here in two constructive versions, used in one and three configurations respectively: copper tube and synthetic capillary tube mats (Fig. 1).

The first constructive version consists of a ceiling in which the copper cooling coils are in direct contact with a smooth perforated metallic surface. The pipe-radiant panel contact must be established in such a way to get a minimum thermal contact resistance; a perforated plate assures suitable convective flow to improve its performance.

The second constructive version uses cooling mats consisting of numerous thin capillary tubes (D_i = 2.3 mm) made in polyethylene and mounted in parallel. The distance between the individual small tubes through which chilled water flows is small enough to ensure that a homogeneous temperature is produced on the bottom side of the ceiling. The cooling mats in this system can be incorporated into the ceiling in three configurations: placed on top of the metal ceiling panels with a layer of mineral wool installed above, embedded into a ceiling plaster layer, or stretched between insulation and gypsum plasterboard (Fig. 2).

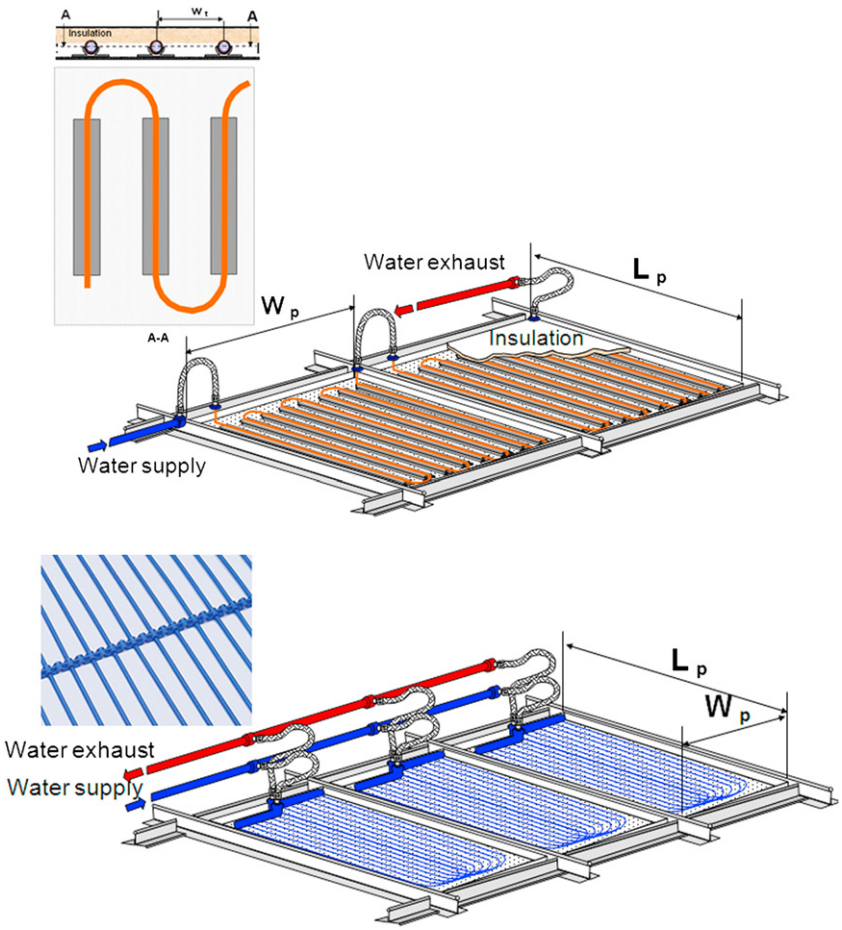

Fig. 1 – Copper tube and synthetic capillary mats cooling ceilings.

The main characteristics of cooling ceilings tested are presented in Table 1.

In this study and for the copper tube cooling ceiling system, the test chamber has been adapted in a way to reproduce as well as possible the characteristics of a real office room. Ten base-type tests are performed with the objective of observing the influences of mass flow rate, supply water temperature, ventilation mode and thermal load distribution on the cooling ceiling capacity and on the comfort conditions. The climatic chamber used is 3.1 m in height, 3.6 m in wide and 6 m in length, with the cooling ceiling located at 2.7 m above the floor. The chamber is connected through its ''façade'' to

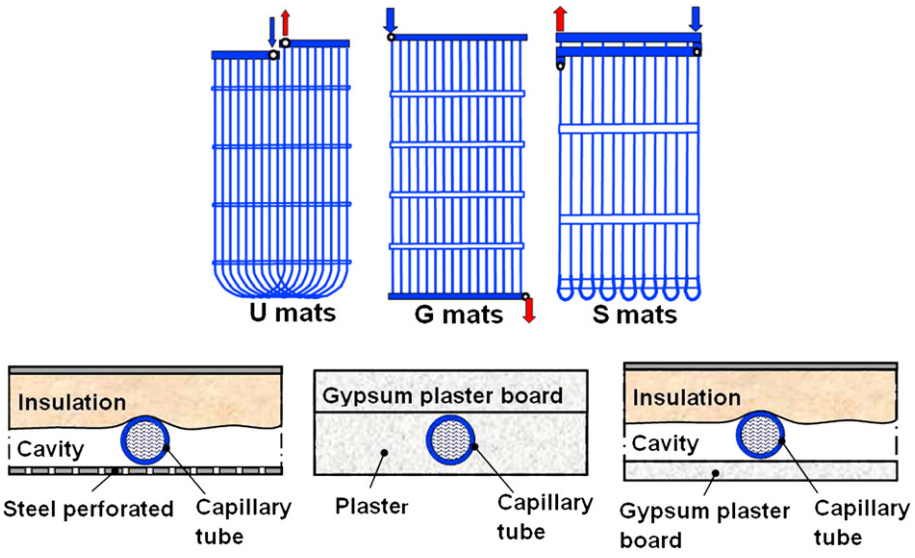

Fig. 2 – Capillary tube mats configurations and radiant surfaces.

Table 1 – Main characteristic of the tested cooling ceilings.

Characteristic	Copper	"U" mats	"S" mats	"G" mats
Radiant surface	On top of a steel plate, thickness 0.8 mm	On top of a steel plate, thickness 0.8 mm	Embedded in plaster, thickness 26 mm	On top of gypsum plasterboard, thickness 10 mm
L_p: panel length	1.15 m	1.37 m	3.5 m	3.7 m
W_p: panel width	1.25 m	0.617 m	0.87 m	0.23 m
w_t: tube separation	100 mm	10 mm	15 mm	10 mm
Panel surface:	1.44 m^2	0.845 m^2	3.06 m^2	0.85 m^2
Perforated area (ρ)	21%	16%	–	–
N_s: panels in series	4	1	1	2
N_p: panels in parallel	2	12	4	6
Upward insulation:	30 mm mineral wool	20 mm mineral wool	–	30 mm mineral wool
Tube-radiant surface union system	Aluminum interconnection profile	Directly placed on top of the plate	Attached below and then plastered in.	Directly placed on top of the board
D_e	13 mm	3.4 mm	3.4 mm	3.4 mm
D_i	12.5 mm	2.3 mm	2.3 mm	2.3 mm

a space to simulating the outdoor environment. It is also surrounded by other controlled spaces in order to avoid any ambient perturbation (Fig. 3 In order to simulate the external thermal load, the "outdoor" space is heated until producing the required load inside the chamber.

Measurements are performed according to ANSI/ASHRAE, 1991 and ANSI/ASHRAE, 1992). The method used here for uncertainty analysis is based on the ASHRAE Guideline 2-2005; instrumental accuracies are given for a confidence level of 95%.

Table 2 gives the combined uncertainties (device and data acquisition system). For the temperatures, two sources of uncertainty are considered: one coming from the thermocouple tolerance (±0.5 K) and the other coming from the data acquisition system (±0.3 K). This gives an overall absolute uncertainty of ±0.6 K (the relative uncertainty is smaller). The air flow rate is measured according to international standard ISO 5167 (1991). The corresponding cooling effect of the air discharged into the chamber is evaluated with an uncertainty of ±3.5%. The AU experimental value is evaluated with an uncertainty of ±5.3%.

For capillary tube mats cooling ceilings, three different radiant surfaces (Fig. 2) are tested in the same test room, according to the standard DIN 4715-1 (1993) (Fig. 4). The main goal of this kind of test is to calculate the cooling ceiling capacity in order to compare differents cooling ceiling configurations. Therefore, a homogeneous load distribution is considered without influence of the ventilation system and of the facade (C. Kochendörfer, 1996).

For this kind of test, the cooling power is measured with an uncertainty of ±3%. Water temperature difference and globe temperature are measured with PT100 sensors with a deviation lower than ±0.02 K and ±0.04 K respectively. The mass flow rate is measured with a magnetic inductive volumetric flow meter with uncertainty of ±0.5% (FTZ, 2002, 2003), (HLK, 1995).

3. Experimental results and analysis

From the thermal balances of the test chamber, the AU value of the copper tube cooling ceiling is calculated as function of the water flow rate $\dot{M}_w$ (varying from 0.0397 kg/s to 0.103 kg/s) and of the log mean temperature difference $\Delta_{T,Ln,center}$ (varying from 7.63 K to 9.95 K) (Eq. (1)–(3)). The resultant temperature used as reference is measured at the center of the chamber at 75 cm from the floor.

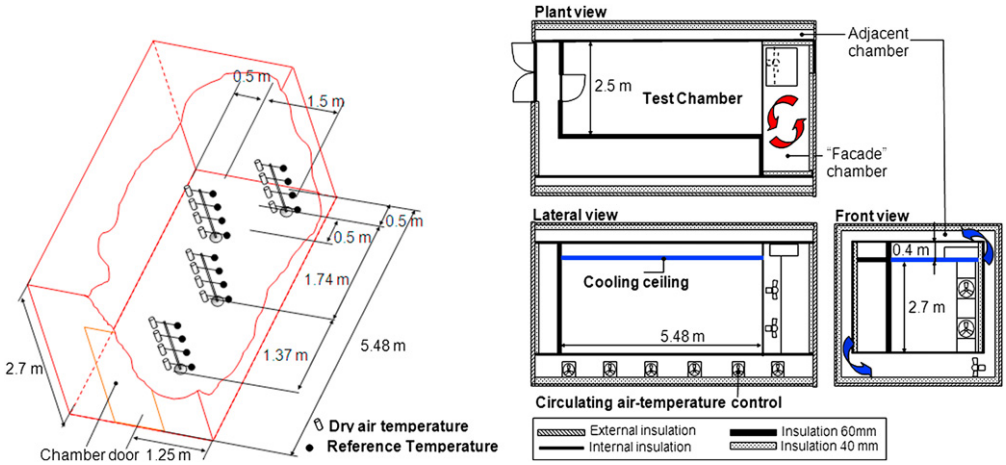

Fig. 3 – Copper tube cooling ceiling test chamber.

Table 2 – Measuring uncertainties.

Variable		Measurement range	Uncertainty
Temperature differentials	ΔT_w	2–5 K	±0.25 K
	ΔT_a	10 K	±0.25 K
Flows	$\dot{M}_w$	0.0397 kg/s–0.103 kg/s	±0.1% of the measured value
	$\dot{M}_a$	96–105 m^3/h	±3.5% of the measured value
Electrical powers	$\dot{W}_f$	290–500 W	±1% of the measured value
	$\dot{W}_{in,loads}$	750–1060 W	±1% of the measured value

$$AU_{center} = \frac{\dot{Q}}{\Delta_{T,Ln,center}} \quad [W/K] \tag{1}$$

$$\dot{Q} = \dot{M}_w \cdot c_{pw} \cdot (t_{w,su} - t_{w,ex}) \quad [W] \tag{2}$$

$$\Delta_{T,Ln,center} = \left| \frac{(t_{w,su} - t_{w,ex})}{\ln\left[\frac{t_{w,su} - t_{res,room,center}}{t_{w,ex} - t_{res,room,center}}\right]} \right| \quad [K] \tag{3}$$

In nominal conditions, an average of 76.7% of the room thermal loads is extracted by the cooling ceiling and 23.3% by the ventilation system. The average heat gains from the ceiling void and from the façade correspond to 10.2% and 38.5% of the total thermal load respectively. The residual of this thermal balance is ±2% of the cooling ceiling capacity. In the experimental domain considered, it is observed that the influence of the three parameters $(\dot{M}_w, \Delta_{T,Ln})$ on AU is negligible. An AU_{center} average value of 106.4 W/K is observed (Table 3). However, this value is significantly affected by the choice of the indoor reference temperature as shown in Table 3: the AU value is reduced when choosing a reference temperature nearer to the frontage. This decrease is reaching 10% when using as reference the globe temperature at 0.5 m from the frontage.

It is observed also that, except for the back side of the chamber, close to the floor, the air velocity into the occupancy zone is always lower than 20 cm/s. This value fulfills the recommended levels of thermal comfort (ASHRAE, 2005; Behne, 1996; Kulpmann, 1993).

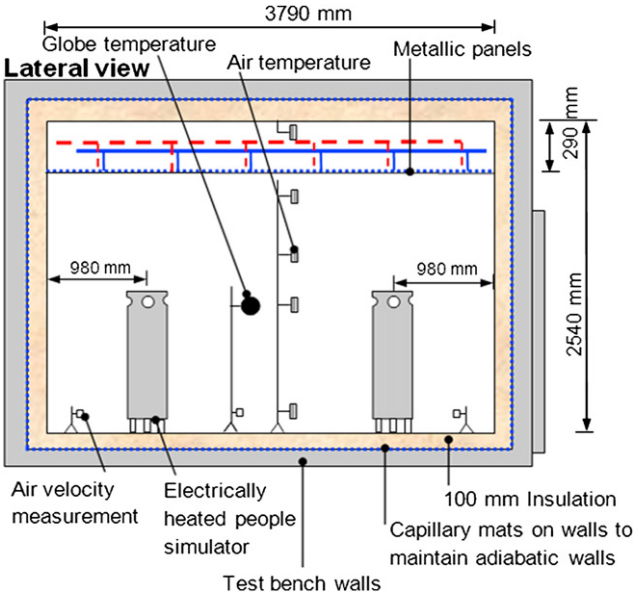

Fig. 4 – Lateral view of test chamber according to DIN 4715-1.

3.1. *Mathematical model description*

3.1.1. *Copper tube cooling ceiling modeling*

An individual element can be defined as shown in Fig. 5. Considering the symmetry between tubes, the applicable boundary conditions are:

1) No heat flow in the fin representing the ceiling at midway between the tubes
2) Ceiling fin base temperature (t_{cc0}) corresponding to the fin temperature immediately below the tube.

On the axial orientation, a nominal tube length of L_{tp} has to be chosen.

The cooling ceiling model is characterized by the inputs, outputs and parameters shown in Fig. 6.

The following basic assumptions are used in the simulation model:

- Uniform air temperature and humidity inside the room
- Steady-state, one-dimension heat transfer
- Mechanical ventilation in the space above the ceiling
- Transition or turbulent flow inside the tubes (design condition).

Heat flow definitions

According to Fig. 5, the total water enthalpy flow rate per unit of length corresponds to the addition of the total thermal energy extracted by the cooling ceiling panel $\dot{Q}'_{CC}$ with the heat gain through the tube external surface from the ceiling cavity $\dot{Q}'_{t,cavity}$:

$$\dot{Q}'_{total} = \dot{Q}'_{CC} + \dot{Q}'_{t,cavity} \tag{4}$$

with:

$$\dot{Q}'_{total} = \frac{t_{w,ave} - t_t}{R'_w + R'_t} \tag{5}$$

And with

$$t_{w,average} = \frac{t_{w,su} + t_{w,ex}}{2} \quad [°C] \tag{6}$$

The total heat flow extracted by the cooling ceiling panel $\dot{Q}'_{CC}$ corresponds to the sum of the heat flows (convection + radiation) coming from the ceiling cavity $\dot{Q}'_{CC,cavity}$ and from the room $\dot{Q}'_{CC,room}$ according to:

Table 3 – AU calculated values using reference temperatures at the center, 1 m and 0.5 m from the façade.

Test	$t_{w,su}$ [°C]	$t_{w,ex}$ [°C]	$t_{res,center}$ [°C]	$t_{res,1m}$ [°C]	$t_{res,0.5m}$ [°C]	$\dot{M}_w$ [kg/s]	AU_{center} [W/K]	AU_{1m} [W/K]	$AU_{0.5m}$ [W/K]
2705b	12.05	15.87	23.9	24.65	24.77	0.0656	107.0	99.28	98.15
2805a	14.04	17.66	25.1	25.97	26.1	0.0638	105.4	96.59	95.34
0206b	14.88	17.03	24.5	25.32	24.77	0.103	109.5	99.45	105.7
0306a	14.89	17.26	24.1	24.93	25.25	0.0856	107.2	96.5	93.1
0306d	14.82	18.7	25	26.04	26.35	0.0519	106.8	94	90.86
0406a	15.68	19.44	25.6	26.62	26.85	0.0532	105.9	93.81	91.42
0506b	14.03	18.87	26.6	27.28	27.28	0.0526	107.1	94.69	100.1
1006a	14.66	19.51	25	25.91	26.21	0.0397	105.7	93.76	90.52
1206b1	14.64	19.41	25.1	25.88	26.46	0.0405	103.8	93.66	87.63
1206c3	14.38	19.4	25	25.85	26.49	0.0394	105.6	94.96	88.31

$$\dot{Q}'_{CC} = \dot{Q}'_{CC,room} + \dot{Q}'_{CC,cavity} \tag{7}$$

The cooling ceiling average temperature is one of the outputs of the model; it can be calculated with reference to the fin effectiveness (Eq. (8)) (Fig. 7).

$$t_{w,average} = t_{a,cc} - \varepsilon_{fin} \cdot (t_{a,cc} - t_{cc,0}) \quad [°C] \tag{8}$$

The air temperature close to the cooling ceiling surface ($t_{a,cc}$) is defined as a weighted average of $t_{a,cavity}$ and $t_{a,room}$; the weighting factors are the heat transfer coefficients:

$$t_{a,cc} = \frac{h_{cc,room} \cdot t_{a,room} + h_{cc,cavity} \cdot t_{a,cavity}}{h_{cc,room} + h_{cc,cavity}} \quad [°C] \tag{9}$$

The cooling ceiling heat transfer coefficient can be defined as:

$$h_{cc} = h_{cc,room} + h_{cc,cavity} \quad [W/m^2K] \tag{10}$$

The temperature distribution along a one-dimensional fin is described by the following equation:

$$\frac{d^2 t_{cc}}{dx^2} = \frac{h_{cc} P}{A_c k_{cc}} (t_{ccaverage} - t_{a,cc}) \tag{11}$$

Where P is the fin perimeter and A_c is the cross-sectional area of the fin (Fig. 8).

The solution of this equation gives the following expression for the fin temperature in a section "x":

$$\frac{t_{cc,x} - t_{a,cc}}{t_{cc,0} - t_{a,cc}} = \frac{\cos h(m \times (L_c - x))}{\cos h(m \times L_c)} \tag{12}$$

with:

$$m^2 = h_{cc} \times \frac{P}{A_c \times k_{cc}} \tag{13}$$

and

$$L_c = \frac{w_t - D_e}{2} \quad [m] \tag{14}$$

The thermal conductivity of the cooling ceiling panel is (k_{cc}) is considered as a model parameter. The effectiveness of this equivalent fin can be defined by Eq. (15).

$$\epsilon_{fin} = \frac{M_f * \tanh(m * L_c)}{h_{CC} * A_f} \tag{15}$$

Where A_f is the surface area of the fin (Fig. 8) and:

$$M_f = \sqrt{h_{cc} \times P \times k_{cc} \times A_c} \tag{16}$$

In the current technical literature, the perforations effect is not considered (ASHRAE, 2004; Kilkis, 1995; Udagawa, 1998; Miriel et al., 2002; Jeon and Mumma, 2004). In this modeling, a simplified approach is used; it is based on the definition of a fin porosity factor ρ. The following effects are considered: environmental heat transfer area, heat conduction inside fin and surface temperature.

The fin geometry can be redefined as:

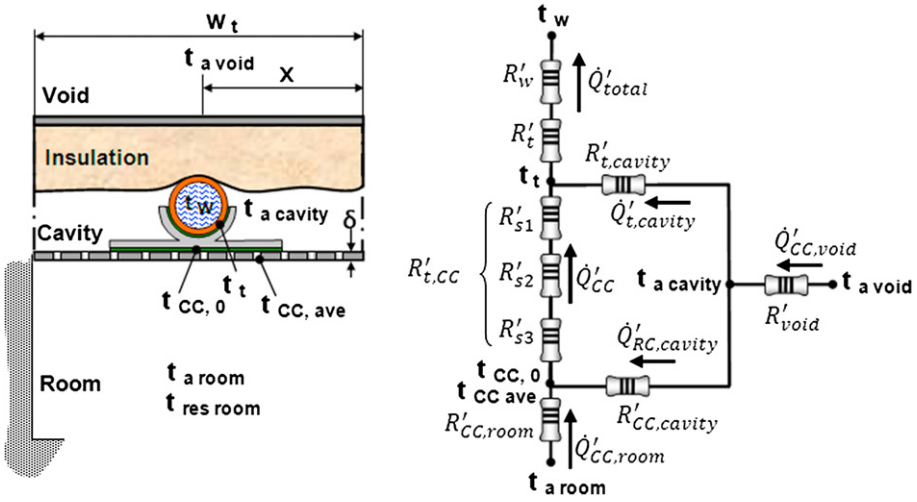

Fig. 5 – Individual copper tube cooling ceiling element and its equivalent thermal circuit.

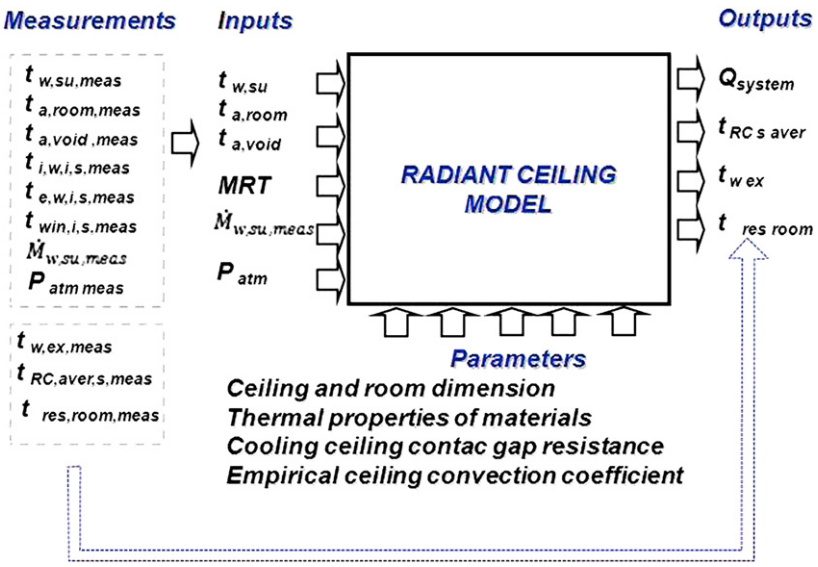

Fig. 6 – Definition of the cooling ceiling model inputs outputs and parameters.

$$P = 2\cdot\left[\frac{\delta_{cc}}{L_{t,p}} + 1\right]\cdot(1+\rho) \quad [-]\ \text{(Per unit of length)} \tag{17}$$

$$A_c = \delta_c\cdot(1-\rho) \quad [\text{m}]\ \text{(Per unit of length)} \tag{18}$$

$$A_f = P\cdot L_c\cdot(1-\rho) \quad [\text{m}]\ \text{(Per unit of length)} \tag{19}$$

The heat gain from ceiling void through the insulation (Fig. 5) can be expressed as a function of the air void temperature (taken as an input in this model) and the void thermal resistance (combination of conduction and convection through the insulation).

Thermal resistance definitions

Water to internal tube surface (R'_w).

$$R'_w = \frac{1}{A_w\cdot h_w} \quad [\text{Km/W}] \tag{20}$$

The order of magnitude for Re_D with the conditions used for experimental validation of the model is 2168 ~ 5743 for the copper tubes (and 4108 ~ 12 214 for the capillary tubes which will be considered later). The Gnielinski equation (Eq. (21)) can be used for forced convection inside tubes in transition or turbulent flow (Celata et al., 2007).

$$Nus_w = \frac{\frac{f_r}{8}(Re-1000)\cdot Pr_w}{1+12.7\left|\frac{f_r}{8}\right|^{1/2}\cdot\left(Pr_w^{2/3}-1\right)} \quad [-] \tag{21}$$

With

$$f_r = (1.82\cdot\log(Re)-1.64)^{-2} \quad [-] \tag{22}$$

$$Re = 4\cdot\frac{\dot{M}_w/N_p}{\pi\cdot D_i\cdot\mu_w} \quad [-] \tag{23}$$

Tube shell (R'_t).

$$R'_t = \frac{\ln\left|\frac{D_e}{D_i}\right|}{2\cdot\pi\cdot k_t} \quad [\text{Km/W}] \tag{24}$$

Cooling ceiling thermal contact resistance ($R'_{t,cc}$). Thermal resistance between tube and ceiling plate is divided into 3 parts (Fig. 5): contact resistance between tube external surface and interconnection profile (R'_{s1} bond contact gap1), conductive resistance through the interconnection profile (R'_{s2}) and contact resistance between interconnection profile and ceiling plate (R'_{s3} bond contact gap2).

The total resistance is:

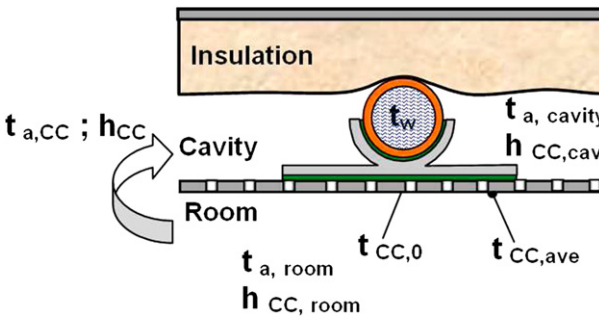

Fig. 7 – Heat transfer and temperature definition on an individual ceiling element as a fin.

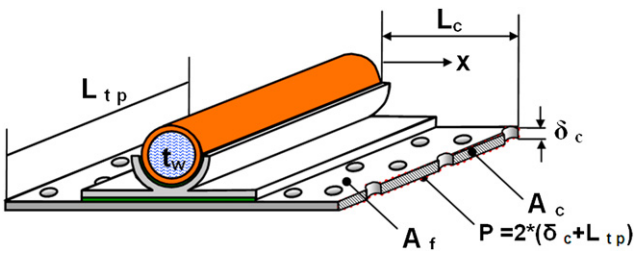

Fig. 8 – Individual ceiling element as a fin.

$$R'_{t,cc} = R'_{s1} + R'_{s2} + R'_{s3} \quad [\mathrm{Km/W}] \tag{25}$$

with:

$$R'_{s1} = \frac{\ln\left|\frac{D_e + 2\cdot\delta_{s1}}{D_e}\right|}{\pi \cdot k_{s1}} \quad [\mathrm{Km/W}] \tag{26}$$

Where δ_{s1} is the bond thickness gap; this parameter is experimentally identified.

As the cross section shape and geometry of the interconnection profiles are difficult to evaluate, a fictitious rectangular cross section is defined for the modeling, with base A_{s2} (contact surface) and thickness δ_{s2} (see Fig. 9):

$$R'_{s2} = \frac{\delta_{s2}}{A_{s2}\cdot k_{s2}} \quad [\mathrm{Km/W}] \tag{27}$$

The net effect of these simplifications on R'_{s2} calculation is relatively small, considering the high thermal conductivity of the interconnection profile (usually made in aluminum).

For R'_{s3}, the same methodology is used, but in this case, it is assumed that:

$$R'_{s3} = \frac{\delta_{s3}}{A_{s3}\cdot k_{s3}} \quad [\mathrm{K\times m/W}] \tag{28}$$

where: $\delta_{s3} = \delta_{s1}$ and $A_{s3} = \delta_{s2}$.

Ceiling plate thermal resistances (as a fin) (R'_{cc}).

$$R'_{cc,cavity} = \frac{1}{h_{cc,cavity}\cdot A_{cc,cavity}} \quad [\mathrm{K\times m/W}] \tag{29}$$

$$R'_{cc,room} = \frac{1}{h_{cc,room}\cdot A_{cc,room}} \quad [\mathrm{K\times m/W}] \tag{30}$$

$A_{cc,cavity}$ and $A_{cc,room}$ are the ceiling element surfaces in contact with the air ceiling cavity and room respectively. A similar approach is used to define the thermal resistance of the tube surface into the ceiling cavity.

Heat transfer coefficient definitions

Ceiling panel to the room ($h_{cc,room}$). Both convection and radiation have to be considered:

$$h_{cc,room} = h_{cc,room,conv} + h_{cc,room,rad} \quad [\mathrm{W/m^2K}] \tag{31}$$

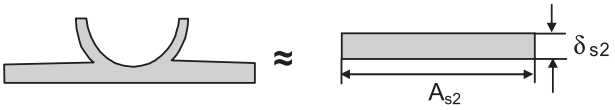

Fig. 9 – Interconnection profile modeling assumption.

Room-ceiling convection ($h_{cc,room,conv}$). For the studied element:

$$h_{cc,room,conv} = \frac{k_a}{L_{c,cc}}Nu_{cc,room} \quad [\mathrm{W/m^2K}] \tag{32}$$

According to what is recommended in ASHRAE System and Equipment Handbook (2004) the following natural convection law (McAdams, 1954) can be used here:

$$Nus_{cc,room} = C_{h,cc,room}\cdot Ra_{cc,room}^{1/n} \quad [-] \tag{33}$$

For pure free convection in a cooled plate facing downwards the coefficient $\mathbf{C_{h,cc,room} = 0.54}$ and $n = 4$ (for $104 \le Ra \le 107$) or $\mathbf{C_{h,cc,room} = 0.15}$ and $n = 3$ (for $107 \le Ra \le 1011$) (Incropera and DeWitt, 1996).

However, among others to make sure that the cooling ceiling system is operates only in dry regime, moisture has usually to be removed from the room through a mechanical ventilation system which generate some air movement.

Because the convective heat transfer is enhanced by both air movement and perforations effects, the use of the natural convection heat transfer coefficient is inappropriate for a mechanically ventilated room. Therefore $C_{h,cc,room}$ is considered here as a model parameter to be identified on the basis of experimental tests.

The convective heat transfer coefficient of the copper tube cooling ceiling tested is currently found in the range of 5.9 ~ 6.5 W/m^{2}K with Ra ≈ 3 × 108 and $C_{h,cc,room}$ = 0.286. This actually corresponds to a very strong enhancement by ventilation and perforations effect.

Room-ceiling radiation ($h_{cc,room,rad}$). In order to analyze the internal radiant exchanges, each surface of the enclosure can be characterized by its uniform radiosity and irradiation. The net radiative heat flux of the ceiling surface can be evaluated by Eqs. (34) and (35) from radiosities (J_i), emissivities (ϵ_i), areas (A_i), view factors ($F_{i,j}$) and black body emissive powers (E_{bi}) (Incropera and DeWitt, 1996):

Table 4 – Experimental and calculated values for copper tube cooling ceiling.

AU [W/K]	AU_{exp} [W/K]	$Error_{AU}$ [W/K]	$\Delta_{T,Ln}$ [K]	$\Delta_{T,Ln,exp}$ [K]	$t_{w,ex,exp}$ [°C]	$t_{w,ex}$ [°C]	$\dot{M}$ [kg/s]	$t_{a,void}$ [°C]	$t_{res,room}$ [°C]	$t_{a,room}$ [°C]	$t_{cc,ave}$ [°C]	$t_{w,su}$ [°C]
107.5	107	−0.479	9.807	9.78	15.87	15.89	0.0656	22.9	23.9	23.8	16.13	12.05
106.4	105.4	−0.961	9.123	9.17	17.66	17.67	0.0638	24.17	25.1	25.1	17.86	14.04
109	109.5	0.458	8.5	8.47	17.03	17.03	0.103	23.97	24.5	24.4	17.79	14.88
107.2	107.2	0.0044	7.96	7.93	17.26	17.27	0.0856	23.38	24.1	24	17.78	14.89
106.9	106.8	−0.105	8.041	8.02	18.7	18.78	0.0519	24.24	25	24.9	18.59	14.82
105.7	105.9	0.208	7.896	7.91	19.44	19.43	0.0532	25.01	25.6	25.5	19.28	15.68
107.2	107.1	−0.144	9.951	9.95	18.87	18.88	0.0526	24.88	26.6	26.7	18.74	14.03
105.3	105.7	0.409	7.66	7.63	19.51	19.51	0.0397	23.97	25	24.9	18.84	14.66
103.5	103.8	0.291	7.829	7.79	19.41	19.42	0.0405	23.9	25.1	25	18.78	14.64
105.9	105.6	−0.330	7.837	7.84	19.4	19.41	0.0394	24.18	25	25	18.73	14.38

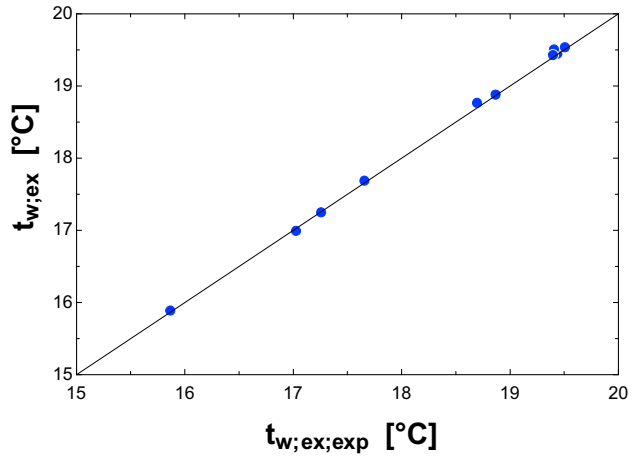

Fig. 10 – Simulated versus measured exhaust water temperature.

$$\dot{Q}_{rad,i} = \sum_{j=1}^{N} A_i.F_{i,j}(J_i - J_j) \tag{34}$$

$$\frac{E_{b,i} - J_i}{\frac{1-\epsilon_i}{\epsilon_i.A_i}} = \sum_{j=1}^{N} A_i.F_{i,j}(J_i - J_j) \tag{35}$$

The net radiant heat flux at the ceiling surface can be determined by solving the unknown J_i. This method supposes that the (supposed-to-be uniform) surface temperatures are known. But surface temperature measuring uncertainties (walls and gazing) could be significant (Fissore and Fonseca, 2007). This is a typical difficulty in the commissioning process.

Several methods have been developed to simplify this calculation. In the "mean radiant temperature" method (MRT), the thermal radiation interchange inside an indoor space is modeled by assuming that the surfaces radiate to a fictitious, finite surface that gives about the same heat flux as the real multi-surface case (Walton, 1980).

When the surface emittances of the enclosure are nearly equal, the fictitious temperature become the area-weighted average uncooled temperature (AUST) widely used at the related literature (Kilkis, 1995; Jeong and Mumma, 2004; ASHRAE System and Equipment, 2004). In this work however, the fictitious temperature considered is the mean radiant temperature. The MRT equation may be written as:

$$\dot{Q}_{cc,room,rad} = A_{cc,effec} \times \sigma \times F_{r,room} \times \left((t_{cc,average} + 273.15)^4 - (t_{mr,room} + 273.15)^4 \right) \quad [W] \tag{36}$$

The mean radiant temperature of the room uncooled surfaces ($t_{mr,room}$) can be calculated by correcting the mean radiant temperature of the room as the cooled ceiling "sees" an environment which excludes its own influence (Ternoveanu et al., 1999):

$$t_{mr,room} = \left[2 \cdot t_{res,room} - t_{a,room} - \frac{A_{cc,s}}{A_{room,f,s}} \times t_{cc,average} \right] \times \frac{1}{1 - \frac{A_{cc,s}}{A_{room,f,s}}} \quad [°C] \tag{37}$$

Eq. (37) is applicable only if: $|t_{mr,room} - t_{a,room}| < 4$ K (Kulpmann, 1993).

The radiation exchange factor ($F_{r,room}$) for any two diffuse, gray surfaces that form an enclosure can be expressed by Eq. (38) (Incropera and DeWitt, 1996):

$$F_{r,room} = \frac{1}{\frac{1}{F_{cc,f}} + \frac{1}{\varepsilon_{cc}} - 1 + \frac{A_{cc,s}}{A_{room,f,s}} \times \left[\frac{1}{\varepsilon_{f,room}} - 1 \right]} \quad [-] \tag{38}$$

where:

$F_{cc,f}$: radiation view factor from ceiling to a room fictitious surface giving an equivalent heat transfer, as in the real multi-surface case (1.0 for flat ceiling ASHRAE, 2004).

$A_{cc,s}$, $A_{room,f,s}$: area of cooling ceiling and fictitious room surface (other than the ceiling). ε_{cc}, and $\varepsilon_{f,room}$: emissivities of the ceiling (**model parameter**) and of the fictitious surface (0.98 (ASHRAE Handbook, 2005)).

The radiation heat transfer coefficient can be expressed finally as follows:

$$h_{cc,room,rad} = \sigma \times F_{r,room} \times \frac{(t_{cc,average} + 273.15)^4 - (t_{mr,room} + 273.15)^4}{t_{cc,average} - t_{mr,room}} \quad [W/m^2K] \tag{39}$$

The current order of magnitude found for $h_{c,room,rad}$ using this methodology is 5.25 W/m^{2}K.

A similar method is used to calculate the heat transfer coefficient between the ceiling and the cavity.

In the case considered, a difference of the order of 4% is found between the results obtained with detailed and simplified methods.

Global heat transfer characteristics

In order to develop an experimental validation of the model, the AU value and water exhaust temperature are calculated by using the ε-**NTU** method:

Table 5 – Cooper tubes cooling ceiling model errors.

Variable	Average error	Standard deviation	Minimal deviation	Maximal deviation	Confidence limits
AU	0.24 W/K	1.5 W/K	−1.53 W/K	3.23 W/K	1.16 W/K −0.69 W/K
$t_{w,ex}$	−0.01 K	0.03 K	−0.06 K	0.05	0.008 K −0.03 K

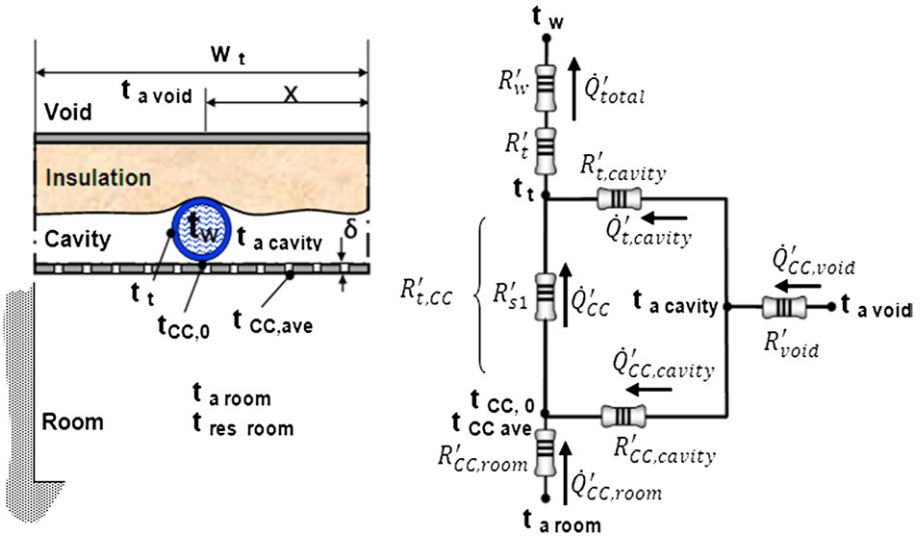

Fig. 11 – Tube mats on top of the metal ceiling panels.

$$AU = \frac{|\dot{Q}_{system}|}{\Delta_{T,Ln}} \quad [W/K] \tag{40}$$

The total heat flow transferred to the water is calculated as follows:

$$\dot{Q}_{system} = \dot{Q}'_{total} \cdot L_{tp} \cdot \frac{W_p \cdot N_p \cdot N_s}{w_t} \quad [W] \tag{41}$$

$$\dot{Q}_{system} = \varepsilon \cdot \dot{M}_w \cdot c_{pw} \cdot (t_{w,su} - t_{res,room}) \quad [W] \tag{42}$$

$$\varepsilon = 1 - \exp(-NTU) \quad [-] \tag{43}$$

$$NTU = \frac{AU}{\dot{C}_w} \quad [-] \tag{44}$$

$$\dot{C}_w = \dot{M}_w \cdot c_{pw}. \quad [W/K] \tag{45}$$

Validation process

The AU experimental values (based on the resultant temperature $t_{res,room}$ measured at the center of the room) are presented in Table 4.

The model parameters are identified with the help of the software EES (Klein and Alvarado, 2001), by minimization of the error function θ, which depends on the relative errors of

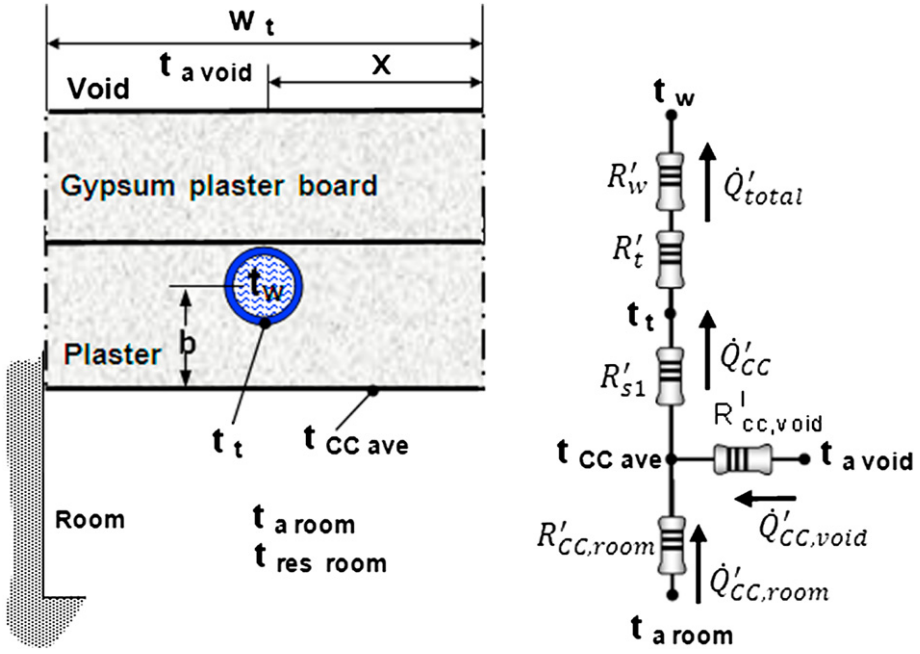

Fig. 12 – Tube mats embedded into the ceiling plaster.

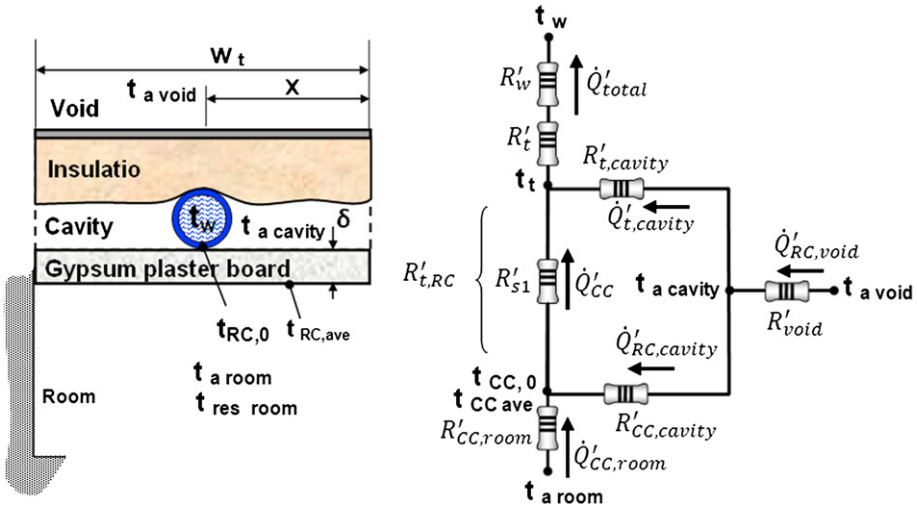

Fig. 13 – Tube mats on top of the gypsum plasterboards.

the following variables: heat transfer coefficients and water exhaust temperatures. This function is defined as follows:

$$\theta = \sqrt{\frac{1}{n}\sum_{j=1}^{m}\sum_{i=1}^{n}\left(\frac{V_{j,i,sim} - V_{j,i,meas}}{V_{j,i,meas}}\right)^2} \quad [-] \tag{46}$$

where V_j is the variable "j", m is the number of variables considered for the minimization and n is the number of tests.

After minimization of the function θ, the following parameters are identified:

$\delta_{s1} = 0.41$ mm (bond thickness gap)
$L_{c,cc} = 0.41$ m (Cooling ceiling characteristic length)
$\varepsilon_{cc} = 0.90$ (Cooling ceiling thermal emissivity)
$k_{cc} = 52$ W/m × K (Cooling Ceiling panel thermal conductivity).

The model results for these conditions are also shown in Fig. 10 and Table 4.

Fig. 10 shows the comparison between measured and simulated exhaust water temperatures.

The model error is here defined with a method similar to that recommended by the ASHRAE Guideline 2 (2005) for experimental data analysis. Average error and standard deviation are defined as follows:

$$\bar{\varepsilon} = \frac{1}{n}\sum_{i=1}^{n}(V_{i,meas} - V_{i,sim}) = \frac{1}{n}\sum_{i=1}^{n}(\varepsilon_i) \quad \sigma = \left[\frac{1}{n}\sum_{i=1}^{n}(\varepsilon_i - \bar{\varepsilon}_i)^2\right]^{0.5} \tag{47}$$

Where $V_{i,meas}$ is the measured variable and $V_{i,sim}$ is the simulated one. The model errors are presented in Table 5. The confidence limits are defined by the following equation:

$$\bar{\varepsilon} \pm \frac{Z\sigma}{\sqrt{n}} \tag{48}$$

with a coefficient $Z = 1.96$ for a probability of 95%.

A good agreement is observed between simulated and measured values.

It is also important to observe that, for this type of cooling ceiling, the values obtained for the heat transfer coefficient (forced convection in tubes with diameters 10 mm, $h_w = 1513$ W/m^{2}K) are much bigger than on air side ($h_{cc,room} = 11.5$ W/m^{2}K). This explains that the AU values presented in Table 4 don't vary very much as function of the mass flow rate.

3.1.2. *Synthetic capillary tube mats cooling ceiling*

The main geometric characteristics of this configuration are summarized in Table 1. An individual element and its equivalent thermal circuit for each tested configuration are shown in Figs. 11–13.

Table 6 – Experimental and calculated values for synthetic capillary tube mats.

Mats	AU [W/K]	AU_{exp} [W/K]	$Error_{AU}$ [W/K]	$\Delta_{T,Ln,exp}$ [K]	$\Delta_{T,Ln}$ [K]	$t_{w,ex,exp}$ [°C]	$t_{w,ex}$ [°C]	$\dot{M}$ [kg/s]	$\dot{q}_{exp}$ [W/m^2]	$t_{w,su}$ [°C]	$t_{a,room}$ [°C]	$t_{a,void}$ [°C]	$t_{res,room}$ [°C]	$t_{cc,average}$ [°C]
U	84.63	84.43	−0.198	6.251	6.25	20.67	20.67	0.1054	52.2	19.47	27.01	22.3	26.34	21.42
	87.61	87.7	0.0832	9.087	9.08	17.82	17.82	0.1053	78.8	16.01	26.85	20.57	26.03	18.95
	90.14	90.2	0.0606	11.77	11.7	16.14	16.14	0.1057	105	13.74	27.7	20.04	26.75	17.64
S	100.4	100.8	0.3874	12.32	12.3	14.78	14.78	0.1088	101.9	12.07	26.2	16.7	25.79	15.43
	96.93	96.83	−0.101	10.01	10.0	16.8	16.81	0.1069	79.6	14.68	26.1	18.1	25.79	17.31
	94.47	95.76	−0.701	7.911	7.91	18.68	18.69	0.1091	62.2	17.02	26.1	19.9	25.79	19.09
G	65.34	64.85	−0.494	6.724	6.72	19.96	19.97	0.0804	42.7	18.67	26.32	22.68	26.06	21.13
	66.55	66.65	0.0961	9.086	9.08	17.85	17.85	0.0807	59.3	16.06	26.34	21.6	26.07	19.44
	68.1	68.55	0.4422	12.13	12.1	15.72	15.72	0.079	81.4	13.22	27.09	21.08	26.64	17.86

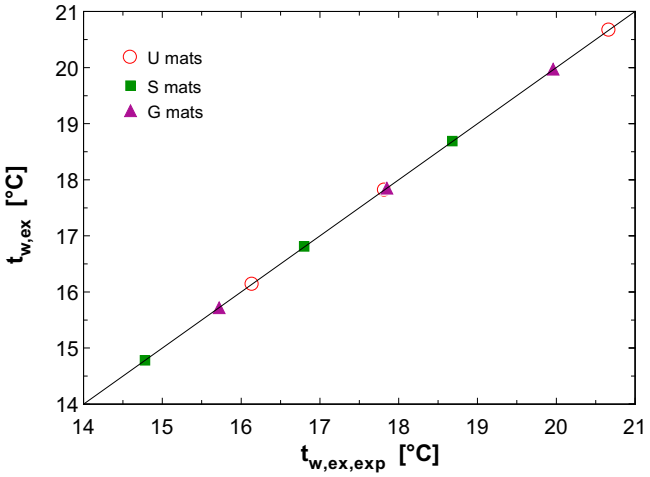

Fig. 14 – Simulated versus measured exhaust water temperature for capillary tube mats cooling ceilings.

Model description

Almost the same model as the copper cooling ceiling is used, with the following changes only:

- For tube mats on top of the metal panels (Fig. 11), the thermal resistance between the tubes and ceiling plate ($R'_{t,cc}$) is reduced to a fictitious thermal resistance (R'_{s1}) through a reduced air layer of thickness δ_{s1}, which is a model parameter to identify on the basis of experimental results.
- For tube mats embedded into the ceiling plaster (Fig. 12), a two-dimensional steady-state conduction heat transfer is considered (according to Rao and Rahmman, 2006; Tadeu and Simoes, 2005; Miriel et al., 2002; Antonopoulos et al., 1997 the time reaction of this kind of cooling ceiling is less than 15 min). The thermal resistance between the tubes and ceiling surface (R'_{s1}) is defined by reference to a horizontal circular cylinder of characteristic length L_{tp}, midway between parallel planes:

$$R'_{s1} = \frac{\ln\left|8\cdot\frac{b}{\pi\cdot D_e}\right|}{2\cdot\pi\cdot k_{s1}} \quad [\mathrm{Km/W}] \tag{49}$$

Where b value is the distance between tube axis and ceiling surface. This term is a model parameter which must be experimentally identified.

- For tube mats on top of the gypsum plasterboards (Fig. 13) there is no air circulation between room and ceiling cavity.

Validation process

The AU experimental value can be calculated as:

$$AU_{exp} = A_{cc,effect}\cdot U_{exp} \quad [\mathrm{W/K}] \tag{50}$$

$$U_{exp} = \dot{q}_{exp}/\Delta_{T,Ln,exp} \quad [\mathrm{W/m^2K}] \tag{51}$$

For the tested mats configurations, the cooling ceiling thermal power $\dot{q}_{exp}$ in W/m^2 is obtained from experimental results according to DIN 4715-1, with constant water mass flow rate and 3 levels of water supply temperature (laboratory reports: FTZ, 2002, 2003 and HLK Stuttgart University, 1995). The experimental log mean temperature difference is also calculated by Eq. (3). The results are shown in Table 6.

Fig. 14 shows the comparison between measured and simulated results of exhaust water temperature.

It is important to consider that for capillary mats cooling ceilings, the experimental tests were performed without ventilation, according to DIN 4715-1 test condition, therefore, $C_{h,cc,room} = 0.15$ and $C_{h,cc,cavity} = 0.27$ (for $Ra = 2.5\times10^7$). After minimization of the error, the model parameters are: For "U" mats configuration $\delta_{s1} = 0.28$ mm, for "S" mats $b = 11.9$ mm and for "G" mats $\delta_{s1} = 0.36$ mm. The model results for these conditions are shown in Table 6.

The model errors are presented in Table 7. A very good agreement is observed between simulated and measured values. It is important to observe that for the capillary tube mats cooling ceiling, the heat transfer coefficients (forced convection in tubes with diameters of 2.3 mm, $h_w = 9341$ W/m^{2}K) are much bigger on water side than on air side ($h_{cc,room} = 8.8$ W/m^{2}K). This makes that, in this case also (and even more), the water flow rate influence on AU value is negligible. But the pressure drop is also important in this case. This makes that pumping energy consumption is no more negligible and can significantly affect the global COP of the cooling system.

Table 7 – Cooper tubes cooling ceiling model errors.

Mats	Variable	Average error	Standard deviation	Minimal deviation	Maximal deviation	Confidence limits
U	AU	−0.018 W/K	0.15 W/K	−0.2 W/K	0.08 W/K	0.15 W/K −0.19 W/K
	$t_{w,ex}$	0.003 K	0.001 K	0.001 K	0.004 K	0.005 K 0.001 K
S	AU	−0.14 W/K	0.54 W/K	−0.7 W/K	0.38 W/K	0.47 W/K −0.75 W/K
	$t_{w,ex}$	−0.007 K	0.002 K	−0.009 K	−0.005 K	−0.005 K −0.009 K
G	AU	−0.015 W/K	0.47 W/K	−0.5 W/K	0.44 W/K	0.51 W/K −0.54 W/K
	$t_{w,ex}$	−0.003 K	0.009 K	−0.001 K	0.003 K	0.007 K −0.013 K

3.2. *Commissioning application*

The steady-state model can support a Functional Performance Test of the system to verify the main cooling ceiling performances (and to compare them with data given in As-Built files). The test consists in measuring the variables defined as model inputs (including the verification measurements, see Fig. 6) and in calculating the cooling ceiling capacity, ceiling surface average temperature and water exhaust temperature. The experimental data provided by the manufacturer can be used in order to identify the model parameters (first parameter identification).

4. Conclusions

The modeling and experimental validation of four different cooling ceiling systems are presented here as a part of the study of the system in cooling mode. A good agreement is found between simulated and measured values. The results show that the average difference between simulated and measured AU value and exhaust water temperature are lower than ± 0.15 W/K and ± 0.01 K respectively.

The theoretical approach gives to the user an appropriate tool for preliminary calculation, design and diagnosis in commissioning processes.

The water flow rate has a small influence on cooling ceiling capacity, but the corresponding pressure drop deserves to be carefully checked.

The experimental results show that the convection heat transfer on cooling ceiling surface can be strongly enhanced by action of the auxiliary ventilation system (normally used with this kind of systems). The influence of heat sources distribution and surfaces temperatures inside the room is considerable. The cooling ceiling must be evaluated together with its designed environment and not as a separate HVAC equipment.

REFERENCES

ANSI/ASHRAE Standard 41.1-1986(RA 91), 1991. Standard Method for Laboratory Airflow Measurement. American Society of Heating, Air-Conditioning and Refrigeration Engineers, Inc, Atlanta.

ANSI/ASHRAE Standard 41.2-1987 (RA 92), 1992. Standard Method for Temperature Measurement. American Society of Heating, Air-Conditioning and Refrigeration Engineers, Inc, Atlanta.

ASHRAE Handbook-HVAC Systems and Equipment, 2004. American Society of Heating, Air-Conditioning and Refrigeration Engineers, Inc, Atlanta (chapter 6).

ASHRAE Handbook, 2005. Fundamentals. American Society of Heating, Air-Conditioning and Refrigeration Engineers, Inc, Atlanta.

ASHRAE Guideline 2, 2005. Engineering Analysis of Experimental Data. American Society of Heating, Refrigerating, and Air-Conditioning Engineers, Inc., Atlanta, USA.

Antonopoulos, A., Vrachopoulos, M., Tzivanidis, C., 1997. Experimental and theoretical studies of space cooling using ceiling embeddes piping. Applied Thermal Engineering 17 (No 4), 351–367.

Behne, M., 1996. Is there a risk of draft in rooms with cooled ceilings. Measurement of air velocities and turbulences. ASHRAE Transactions: Symposia, 744–751. SD 96-4-5.

Celata, P., Cumo, M., McPhail, J., Zummo, G., 2007. Single-phase laminar and turbulent heat transfer in smooth and rough microtubes. Microfluid Nanofluids 3, 697–707.

Conroy, C., Mumma, S., 2005. Ceiling radiant cooling panels as a viable distributed parallel sensible cooling technology integrated with dedicated outdoor air systems. ASHRAE Transactions 107 Part 1 AT-01-7-5.

DIN 4715-1, 1993. Entwurf, Raumkühlflächen; Leistungmessung bei freier Strömung. Prüfregeln, Beuth Verlag GmbH, Berlin.

Feustel, H., Stetiu, C., 1995. Hydronic radiant cooling- preliminary assessment. Energy and Building 22, 193–205.

Fissore, A., Fonseca, N., 2007. Experimental study of the thermal balance of a window, design description. Building and Environment 42, 3309–3321.

FTZ Forschungs-und Transferzentrum e.V and der Westsächsischen Hochschule Zwickau (FH).2002, 2003. Prüfbericht über die Ermittung der Kühlleistung einer Raumkühfläche nach DIN 4715-1. Prüfberich Nr.:FTZ_2003_KF1022.

HLK Heizung Lüftung Klimatechnik Prüfstelle. University of Stuttgar. 1995. Prüfbericht über die Ermittung der Kühlleistung einer Raumkühfläche nach DIN 4715-1. Prüfberich Nr.:VR95 K29. 1134.

Incropera, F., DeWitt, D., 1996. Fundamentals of Heat and Mass Transfer, Fourth ed. School of Mechanical Engineering Purdue University.

ISO 5167-1, 1991. Measurement of Fluid Flow by Means of Pressure Differential Devices Part 1: Orifice Plates, Nozzles and Venturi Tubes Inserted in Circular Cross-section Conduits Running Full. International Organization for Standardization, Geneva.

Jeong, Jae-Weon, Mumma, S., 2004. Simplified cooling capacity estimation model for top insulated metal ceiling radiant cooling panels. Applied Thermal Engineering 24, 2055–2072.

Kilkis, B., 1995. Coolp: a computed program for the design and analysis of ceiling cooling panles. ASHRAE Transaction: Symposia, 705–710. SD 95-4-4.

Klein, S., Alvarado, F., 2001. EES – Engineering Equation Solver, Version 6.045. F-chart Software, Wisconsin (USA).

Kochendörfer, 1996. Standard testing of cooling panels and their use in system planning. ASHRAE Transactions 102 (1), 651–658.

Kulpmann, R., 1993. Thermal comfort and air quality in rooms with cooled ceilings – results of scientific investigations. ASHRAE Transactions: Symposia, 488–502. DE 93 – 2 – 2.

McAdams, H., 1954. Heat Transmission, third ed. Mc Graw-Hill, New York (chapter 7).

Miriel, J., Serres, L., Trombe, A., 2002. Radiant ceiling panel heating-cooling systems: experimental and simulated study of the performances, thermal comfort and energy consumptions. Applied Thermal Engineering 22, 1861–1873.

Rao, C., Rahmman, M., 2006. Transient conjugate heat transfer model for circular tubes inside a rectangular substrate. Journal of Thermophysics and Heat Transfer 20, 122–134.

Ternoveanu, A., Hannay, C., Qingping, W., 1999. Preliminary Analysis on a Research Project for Cooling Ceilings – Synthesis of Available Information. Laboratoire de Thermodynamique appliquée Université de Liège.

Tadeu, A., Simoes, N., 2005. Transient conduction and convection phenomena across a solid layer structure with thermal heterogeneities. Journal of Computer Modeling in Engineering and Sciences, 477–495. CMES 2.

Udagawa, M., 1998. Simulation of panel cooling systems with linear subsystem model. ASHRAE Transaction: Symposia, 534–547. DE 98-3-2.

Walton, G., 1980. A new algorithm for radiant interchange in room loads calculations. ASHRAE Transaction 86 (2), 190–208.